Dzyaloshinskii-Moriya interaction in the presence of Rashba and Dresselhaus spin-orbit coupling

Mohammad M. Valizadeh* and S. Satpathy
Department of Physics and Astronomy, University of Missouri, Columbia, Missouri 65211, USA

(Received 9 December 2017; revised manuscript received 9 February 2018; published 19 March 2018)

Chiral order in magnetic structures is currently an area of considerable interest and leads to skyrmion structures and domain walls with certain chirality. The chiral structure originates from the Dzyaloshinskii-Moriya interaction caused by broken inversion symmetry and the spin-orbit interaction. In addition to the Rashba or Dresselhaus interactions, there may also exist substantial spin polarization in magnetic thin films. Here, we study the exchange interaction between two localized magnetic moments in the spin-polarized electron gas with both Rashba and Dresselhaus spin-orbit interaction present. Analytical expressions are found in certain limits in addition to what is known in the literature. The stability of the Bloch and Néel domain walls in magnetic thin films is discussed in light of our results.

DOI: 10.1103/PhysRevB.97.094419

I. INTRODUCTION

The indirect exchange interaction between two localized magnetic moments, known as the Ruderman-Kittel-Kasuya-Yosida (RKKY) interaction [1–3], has been studied for a long time. This interaction, which has the Heisenberg form of $E = J\vec{S}_1 \cdot \vec{S}_2$, was originally developed for systems without any broken symmetry or spin-orbit coupling (SOC). Dzyaloshinskii and Moriya [4,5] showed that in addition to this scalar interaction, vector and tensor interactions of the types $\vec{D} \cdot \vec{S}_1 \times \vec{S}_2$ and $\vec{S}_1 \cdot \overleftrightarrow{\Gamma} \cdot \vec{S}_2$, respectively, can result in a solid, where both the inversion symmetry is broken and the SOC is present.

The Dzyaloshinskii-Moriya interaction (DMI) is of considerable current interest because of the chiral magnetic states that it can produce, which are an important ingredient, for example, in the formation of skyrmion states as well as the helical spin structures in magnetic bilayers. Recent experiments have shown that the nature of the magnetic domain walls in ultrathin magnetic films depends on the DMI, and furthermore, they can be switched from one type to another via interface engineering [6]. Similarly, another recent experiment has shown that the skyrmion state can be tuned by altering the DMI by varying the magnetic layer compositions [7].

The Rashba [8] and Dresselhaus [9] SOC terms, present due to the surface and bulk inversion asymmetries, respectively, lead in turn to the DMI, which is the subject of this paper. Recently, experimenters [6,7,10–13] were able to tune the strength of the DMI using quantum well structures and/or gate voltage, which leads in turn to the tuning of the magnetic exchange interactions between neighboring spins. Interestingly, Chen *et al.* have shown that by tuning the DMI, the chirality of the magnetic domain walls can be altered [6]. Another motivation for the present work is the Dutta-Das spin transistor [14], where the strength of the Rashba interaction can be controlled by a gate voltage, with potential applications in spintronics.

*mvbr5@mail.missouri.edu

There were several earlier studies of the DMI in the presence of the Rashba and Dresselhaus SOCs, usually when either one or the other is present. In an earlier work, Imamura *et al.* [15] studied the DMI in the presence of the Rashba term, followed by Lyu *et al.* [11] and Mross and Johannesson [16]. Chesi and Loss [17] included the Dresselhaus term and obtained the DMI in certain limits. All of these studies are for a nonmagnetic host material, so that the host electrons are not spin polarized. For the case where spin polarization is present, as in magnetic thin-film structures, very little work has been done, and to our knowledge, just two papers have treated this case and only in the presence of the Rashba term [18,19]. In this paper, we study the DMI in a two-dimensional electron gas (2DEG) with both Rashba and Dresselhaus spin-orbit couplings present along with spin polarization of the electron gas.

II. FORMALISM

We consider a 2D spin-polarized electron gas in the presence of Rashba and Dresselhaus spin-orbit interaction, which is relevant, for example, for a magnetic thin film with bulk and/or surface broken inversion symmetries. The broken bulk inversion symmetry produces the Dresselhaus term, while the surface asymmetry produces the Rashba term, and recently, it was possible [12] to tune the relative magnitudes of the two terms experimentally in semiconductor quantum wells via interface engineering. With both Rashba and Dresselhaus terms present, the system is described by the Hamiltonian

$$\mathcal{H} = \frac{\hbar^2 k^2}{2m}\sigma_0 + \alpha(k_y\sigma_x - k_x\sigma_y) + \beta(k_x\sigma_x - k_y\sigma_y) + \Delta\sigma_z, \tag{1}$$

where α and β are, respectively, the strengths of the Rashba and Dresselhaus terms, σ_i are the Pauli matrices, σ_0 is the unit 2×2 matrix, $\vec{k}$ is the electron momentum, and Δ describes the Zeeman spin splitting of the electron states.

General formalism. We are interested in the magnetic interaction between two localized moments, $\vec{S}_1$ and $\vec{S}_2$, which are embedded in the host electrons and treated as classical

 ©2018 American Physical Society

spins. The localized moments interact with the host electrons via the following contact interaction:

$$V_i(\vec{r}) = -\lambda\delta(\vec{r} - \vec{R}_i)\vec{S}_i \cdot \vec{s}, \quad (2)$$

where $\vec{R}_1 = 0$ and $\vec{R}_2 = \vec{R}$ are the positions of the two moments and $\vec{s} = \hbar\vec{\sigma}/2$.

The magnetic interaction is conveniently expressed as integrals over the expansion coefficients of the Green's functions (GFs) in terms of the Dirac matrices. Below we derive these results, which are true for any general case irrespective of the dimensionality of the system.

The interaction energy $E(\vec{R})$ between the two moments is given by the well-known expression [20]

$$E(\vec{R}) = \frac{-\lambda^2}{\pi} \,\mathrm{Im} \int_{-\infty}^{E_F} \mathrm{Tr}[G(0,\vec{R},E)\, \vec{S}_2 \cdot \vec{s} \times G(\vec{R},0,E)\vec{S}_1 \cdot \vec{s}]dE, \quad (3)$$

where $G(E) = (E + i\eta - \mathcal{H})^{-1}$, with $\eta \to 0^+$, is the retarded GF and E_F is the Fermi energy. The Zeeman term in Eq. (1) introduces a net spin polarization in the electron gas for $\Delta \neq 0$, leading to a constant shift in energy given by

$$E_0 = -\frac{\lambda\hbar}{2}(S_{1z} + S_{2z})(n_\uparrow - n_\downarrow). \quad (4)$$

The spin polarization $n_\uparrow - n_\downarrow$ depends on the system, and for the 2DEG under study here, it is easily shown to be $n_\uparrow - n_\downarrow = 4\pi(2m)^{1/2}\hbar^{-1}[(E_F + \Delta)^{1/2} - (E_F - \Delta)^{1/2}]$, e.g., from the wave functions given later in Eq. (13). Including this energy shift, the total energy becomes

$$E = E_0 + E(\vec{R}) + O(\lambda^3). \quad (5)$$

The GFs in Eq. (3) are 2×2 matrices in spin space with the matrix elements given by

$$G_{\sigma_1\sigma_2}(\vec{r}_1,\vec{r}_2,E) = \sum_{\vec{k}\nu}^{\infty} \frac{\psi_{\vec{k}\nu}(\vec{r}_1,\sigma_1)\psi^*_{\vec{k}\nu}(\vec{r}_2,\sigma_2)}{E + i\eta - \varepsilon_{\vec{k}\nu}}, \quad (6)$$

where $G_{\sigma_1\sigma_2}(\vec{r}_1,\vec{r}_2,E) \equiv \langle\vec{r}_1\sigma_1|\hat{G}(E)|\vec{r}_2\sigma_2\rangle$, $\psi_{\vec{k}\nu}(\vec{r},\sigma) = \langle\vec{r}\sigma|\vec{k}\nu\rangle$, and $\vec{k}\nu$ labels the eigenstates of the system.

It is convenient to write the GFs in terms of the Pauli matrices and express the interaction energy (3) in terms of the trace of products of the Pauli matrices. We thus have

$$G(\vec{R},0,E) = g_0\sigma_0 + \sum_{i=1}^{3} g_i\, \sigma_i,$$
$$G(0,\vec{R},E) = g'_0\sigma_0 + \sum_{i=1}^{3} g'_i\, \sigma_i, \quad (7)$$

where the two GFs are different if we do not have inversion symmetry, which is true for the present case. Using the trace identities

$$\mathrm{Tr}(\sigma_i\sigma_j) = 2\delta_{ij},$$
$$\mathrm{Tr}(\sigma_i\sigma_j\sigma_k) = 2i\varepsilon_{ijk}, \quad (8)$$
$$\mathrm{Tr}(\sigma_i\sigma_j\sigma_k\sigma_l) = 2(\delta_{ij}\delta_{kl} - \delta_{ik}\delta_{jl} + \delta_{il}\delta_{jk}),$$

where δ_{ij} are the Kronecker deltas and ε_{ijk} are the Levi-Civita symbols, it is straightforward to evaluate the interaction energy (3), which yields

$$E(\vec{R}) = J\vec{S}_1 \cdot \vec{S}_2 + \vec{D} \cdot \vec{S}_1 \times \vec{S}_2 + \vec{S}_1 \cdot \overleftrightarrow{\Gamma} \cdot \vec{S}_2. \quad (9)$$

Defining vectors $\vec{g} = \sum_{i=1}^{3} g_i\hat{i}$ and $\vec{g}' = \sum_{i=1}^{3} g'_i\hat{i}$, the expressions for the RKKY and the Dzyaloshinskii-Moriya interaction constants are written as

$$J = \frac{-\lambda^2\,\hbar^2}{2\pi}\int_{-\infty}^{E_F} \mathrm{Im}\,(g'_0 g_0 - \vec{g}'\cdot\vec{g})dE,$$
$$\vec{D} = \frac{-\lambda^2\,\hbar^2}{2\pi}\int_{-\infty}^{E_F} \mathrm{Re}\,(g'_0\,\vec{g} - g_0\,\vec{g}')dE, \quad (10)$$
$$\overleftrightarrow{\Gamma} = \frac{-\lambda^2\,\hbar^2}{2\pi}\int_{-\infty}^{E_F} \mathrm{Im}\,(\vec{g}\,\vec{g}' + \vec{g}'\,\vec{g})dE.$$

The problem thus boils down to the calculation of the GF coefficients $(g_0,\vec{g},g'_0,\vec{g}')$ for the given Hamiltonian.

These equations represent a central result of this paper. They are valid quite generally, i.e., for any system with a 2×2 spin Hamiltonian matrix, irrespective of the dimensionality of the system.

Note that if the inversion symmetry is present, e.g., when the Rashba and Dresselhaus terms α and β are zero, we have $G(\vec{R},0,E) = G(0,\vec{R},E)$, so that $g_0 = g'_0$ and $\vec{g} = \vec{g}'$. In this case, Eq. (10) immediately leads to the well-known result $\vec{D} = 0$, i.e., the absence of the DM interaction for a system with inversion symmetry.

Simplified expressions for the 2DEG. For the 2DEG described by the Hamiltonian (1), the calculation becomes a bit simplified due to the fact that

$$g'_0 = g_0, \quad g'_1 = -g_1, \quad g'_2 = -g_2, \quad g'_3 = g_3. \quad (11)$$

This can be easily proved. To show this, we find the eigenvalues of Hamiltonian (1), which read

$$\varepsilon_\nu(\vec{k}) = \frac{\hbar^2k^2}{2m} + (-1)^\nu[\Delta^2 + (\alpha^2 + \beta^2 + 2\alpha\beta\sin 2\theta)k^2]^{1/2}, \quad (12)$$

where $\nu = 1,2$ is the band index and θ is the polar angle in k space, $\theta = \tan^{-1}(k_y/k_x)$, and the corresponding eigenfunctions are

$$|\vec{k}\nu\rangle = \begin{pmatrix} a^\uparrow_{\vec{k}\nu} \\ a^\downarrow_{\vec{k}\nu} \end{pmatrix},$$
$$a^\uparrow_{\vec{k}\nu} = \Lambda_{\vec{k},\nu}(1 + |\Lambda_{\vec{k},\nu}|^2)^{-1/2},$$
$$a^\downarrow_{\vec{k}\nu} = (1 + |\Lambda_{\vec{k},\nu}|^2)^{-1/2}, \quad (13)$$
$$\Lambda_{\vec{k},\nu} = \frac{i[\Delta + (-1)^\nu\sqrt{\Delta^2 + (\alpha^2 + \beta^2 + 2\alpha\beta\sin 2\theta)k^2}]}{k(\alpha e^{i\theta} + i\beta\, e^{-i\theta})}.$$

The GFs, $G(\vec{R},0,E)$ and $G(0,\vec{R},E)$, can be obtained from Eq. (6), which becomes

$$G_{\sigma_1\sigma_2}(\vec{r}_1,\vec{r}_2,E) = \frac{1}{A}\sum_{\vec{k}\nu} \frac{e^{i\vec{k}\cdot(\vec{r}_1-\vec{r}_2)}a^{\sigma_1}_{\vec{k}\nu}a^{\sigma_2 *}_{\vec{k}\nu}}{E + i\eta - \varepsilon_{\vec{k}\nu}}, \quad (14)$$

with A being the area of the 2D space. From Eqs. (12) and (13) and the fact that changing $\vec{k}$ to $-\vec{k}$ is equivalent to changing the polar angle θ to $\theta+\pi$, one readily finds the following equalities:

$$\varepsilon_\nu(\vec{k})=\varepsilon_\nu(-\vec{k}),\quad a^{\uparrow}_{\vec{k}\nu}=-a^{\uparrow}_{-\vec{k}\nu},\quad a^{\downarrow}_{\vec{k}\nu}=a^{\downarrow}_{-\vec{k}\nu}. \tag{15}$$

Using these results, it is easy to see that if we interchange $\vec{r}_1$ and $\vec{r}_2$ and change the dummy index $\vec{k}$ to $-\vec{k}$ in Eq. (14), the spin-diagonal part of the GF remains unchanged, while the off-diagonal part changes sign, viz.,

$$\begin{aligned}G_{\sigma\sigma}(\vec{r}_1,\vec{r}_2,E)&=G_{\sigma\sigma}(\vec{r}_2,\vec{r}_1,E),\\ G_{\sigma\sigma'}(\vec{r}_1,\vec{r}_2,E)&=-G_{\sigma\sigma'}(\vec{r}_2,\vec{r}_1,E).\end{aligned} \tag{16}$$

Note that this is not a general result but is valid only for specific spin texture of the wave function, and the conditions Eq. (15) must be satisfied under momentum inversion. Setting $\vec{r}_2=\vec{R}$ and $\vec{r}_1=0$ and substituting this equation into Eq. (7), we readily find our desired result for the GF coefficients, Eq. (11).

The expressions for the RKKY and the Dzyaloshinskii-Moriya interaction constants, Eq. (10), simplify to

$$J=-\bar{\lambda}\int_{-\infty}^{E_F}\mathrm{Im}\left(g_0^2+g_1^2+g_2^2-g_3^2\right)dE, \tag{17}$$

$\vec{D}=(D_x,D_y,0)$, with

$$\begin{aligned}D_x&=-\bar{\lambda}\int_{-\infty}^{E_F}\mathrm{Re}(2g_0g_1)dE,\\ D_y&=-\bar{\lambda}\int_{-\infty}^{E_F}\mathrm{Re}(2g_0g_2)dE,\end{aligned} \tag{18}$$

and finally,

$$\overleftrightarrow{\Gamma}=\begin{pmatrix}\gamma_{xx}&\gamma_{xy}&0\\ \gamma_{yx}&\gamma_{yy}&0\\ 0&0&\gamma_{zz}\end{pmatrix}, \tag{19}$$

with

$$\begin{aligned}\gamma_{xx}&=\bar{\lambda}\int_{-\infty}^{E_F}\mathrm{Im}\left(2g_1^2\right)dE,\\ \gamma_{yy}&=\bar{\lambda}\int_{-\infty}^{E_F}\mathrm{Im}\left(2g_2^2\right)dE,\\ \gamma_{zz}&=-\bar{\lambda}\int_{-\infty}^{E_F}\mathrm{Im}\left(2g_3^2\right)dE,\\ \gamma_{xy}&=\gamma_{yx}=\bar{\lambda}\int_{-\infty}^{E_F}\mathrm{Im}(2g_1g_2)\,dE,\end{aligned} \tag{20}$$

where $\bar{\lambda}\equiv(2\pi)^{-1}\lambda^2\hbar^2$. Note that the GF coefficients g_0 and g_i are functions of $\vec{R}$ and E, being expansions of $G(\vec{R},0,E)$. In the next sections, we use expressions (17)–(20) to evaluate the magnetic interactions in the 2DEG described by the Hamiltonian (1).

III. 2DEG WITH RASHBA SPIN-ORBIT COUPLING

We consider first a 2DEG where only the Rashba interaction is present, with the remaining interactions (Zeeman and Dresselhaus) being zero ($\beta=\Delta=0$). This is an important case found in many situations such as the semiconductor quantum wells [21] and oxide surfaces [22]. Diagonalizing the Hamiltonian (1) for this case

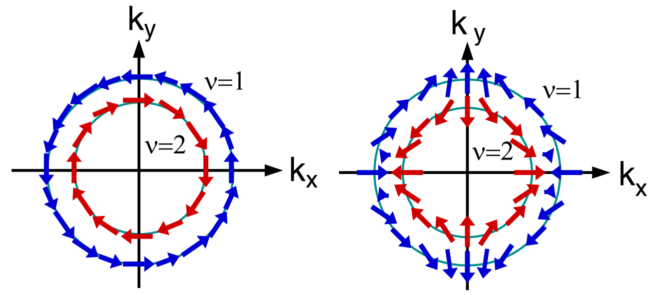

FIG. 1. Spin eigenfunctions for the 2DEG with Rashba (left) and Dresselhaus (right) spin-orbit coupling.

$$H(\vec{k})=\begin{pmatrix}\frac{\hbar^2k^2}{2m}&i\alpha ke^{-i\theta}\\ -i\alpha ke^{i\theta}&\frac{\hbar^2k^2}{2m}\end{pmatrix}, \tag{21}$$

we have the eigenvalues and the eigenfunctions: $\varepsilon_{\vec{k}\nu}=\hbar^2k^2/2m\pm\alpha k$, $a^{\uparrow}_{\vec{k}\nu}=\frac{i}{\sqrt{2}}(-1)^\nu e^{-i\theta}$, and $a^{\downarrow}_{\vec{k}\nu}=\frac{1}{\sqrt{2}}$ for bands $\nu=1$ and 2, and $\theta=\tan^{-1}(k_y/k_x)$, again, is the polar angle in momentum space. The spin eigenfunctions are indicated in Fig. 1. From Eq. (6), the GF matrix elements $G_{\sigma\sigma'}(\vec{r}_1,\vec{r}_2,E)$ are

$$\begin{aligned}G_{\uparrow\uparrow}&=G_{\downarrow\downarrow}=\frac{1}{2A}\sum_{\vec{k}}e^{i\vec{k}\cdot(\vec{r}_1-\vec{r}_2)}\left(\frac{1}{\varepsilon_+}+\frac{1}{\varepsilon_-}\right),\\ G_{\uparrow\downarrow}&=\frac{i}{2A}\sum_{\vec{k}}e^{i\vec{k}\cdot(\vec{r}_1-\vec{r}_2)}e^{-i\theta}\left(\frac{1}{\varepsilon_+}-\frac{1}{\varepsilon_-}\right),\\ G_{\downarrow\uparrow}&=-\frac{i}{2A}\sum_{\vec{k}}e^{i\vec{k}\cdot(\vec{r}_1-\vec{r}_2)}e^{i\theta}\left(\frac{1}{\varepsilon_+}-\frac{1}{\varepsilon_-}\right),\end{aligned} \tag{22}$$

where

$$\varepsilon_\pm=E+i\mu-(\hbar^2k^2/2m\pm\alpha k). \tag{23}$$

The summations can be performed to yield the GF expansion coefficients g_i by changing the summations into integrations and using the Jacobi-Anger expansion [23]

$$e^{i\vec{k}\cdot(\vec{r}_1-\vec{r}_2)}=J_0(k|\vec{r}_1-\vec{r}_2|)+2\sum_{n=1}^{\infty}i^nJ_n(k|\vec{r}_1-\vec{r}_2|)\cos(n\phi), \tag{24}$$

where $J_n(x)$ is the nth-order Bessel function and ϕ is the angle between $\vec{r}_1-\vec{r}_2$ and $\vec{k}$. Since we have the rotational symmetry in the plane [the Rashba term can be written as $(\vec{k}\times\hat{z})\cdot\vec{\sigma}$, so that $\hat{z}$ is the only unique axis], we can choose k_x along $\vec{r}_1-\vec{r}_2$ without any loss of generality. Thus $\phi=\theta$, and performing the angular integrations in Eq. (22) yields the GFs in terms of the Bessel functions, viz.,

$$\begin{aligned}G_{\sigma\sigma}(\vec{r}_1,\vec{r}_2,E)&=\frac{1}{4\pi}\int_0^\infty kJ_0(k|\vec{r}_1-\vec{r}_2|)\left(\frac{1}{\varepsilon_+}+\frac{1}{\varepsilon_-}\right),\\ G_{\uparrow\downarrow}(\vec{r}_1,\vec{r}_2,E)&=-\frac{1}{4\pi}\int_0^\infty kJ_1(k|\vec{r}_1-\vec{r}_2|)\left(\frac{1}{\varepsilon_+}-\frac{1}{\varepsilon_-}\right),\\ G_{\downarrow\uparrow}(\vec{r}_1,\vec{r}_2,E)&=-G_{\uparrow\downarrow}(\vec{r}_1,\vec{r}_2,E).\end{aligned} \tag{25}$$

The diagonal elements are the same, while the off-diagonal elements differ by a sign, which leads to the form $G(\vec{R},0,E) = g_0\sigma_0 + g_2\sigma_2$, with g_1 and g_3 both being zero. One can similarly evaluate $G(0,\vec{R},E) = g_0\sigma_0 - g_2\sigma_2$, so that $G(\vec{R},0,E) \neq G(0,\vec{R},E)$, a result consistent with the broken inversion symmetry. The momentum integrations in Eq. (25), after some algebra, yield the coefficients

$$g_0 = -\frac{i\,m}{4\hbar^2}\left(\frac{f(\alpha,E)+\alpha}{f(\alpha,E)}H_0^{(1)}\left\{\frac{m}{\hbar^2}[f(\alpha,E)+\alpha]R\right\} + \frac{f(\alpha,E)-\alpha}{f(\alpha,E)}H_0^{(1)}\left\{\frac{m}{\hbar^2}[f(\alpha,E)-\alpha]R\right\}\right),$$
$$g_2 = \frac{m}{4\hbar^2}\left(\frac{f(\alpha,E)+\alpha}{f(\alpha,E)}H_1^{(1)}\left\{\frac{m}{\hbar^2}[f(\alpha,E)+\alpha]R\right\} - \frac{f(\alpha,E)-\alpha}{f(\alpha,E)}H_1^{(1)}\left\{\frac{m}{\hbar^2}[f(\alpha,E)-\alpha]R\right\}\right), \quad (26)$$

where $f(\alpha,E) = \sqrt{\alpha^2 + \frac{2\hbar^2}{m}E}$ and $H_n^{(1)}(x)$ are the Hankel functions of the first kind and order n.

The magnetic interactions J, $\vec{D}$, and $\overleftrightarrow{\Gamma}$ are obtained from Eqs. (17)–(19) and (26), and in light of the fact that only g_0 and g_2 are nonzero, this in turn makes only J, D_y, and γ_{yy} nonzero, with all other components being zero. These can be computed numerically in general, but for specific limits, approximate results may be obtained analytically, which we explore below.

It is straightforward to take the limit of the Rashba SOC going to zero ($\alpha = 0$) in Eq. (26) and obtain the well-known results for J for the standard electron gas in two dimensions [24].

It is instructive to show explicitly the rotational invariance of the interaction energy $E(\vec{R})$; that is, if we rotate the position of the spin $\vec{R}$ as well as $\vec{S}_1,\vec{S}_2$ about the $\hat{z}$ axis, then the energy will not change, even though the individual interaction parameters might. This is true only if we have rotational symmetry in the plane, which is the case for the Rashba interaction.

To this end, we choose $\vec{R} \equiv \vec{r}_2 - \vec{r}_1$ along the direction with polar angle γ in the k_x-k_y plane and compute the coefficients g_i, which now depend on γ. The results, expressed in terms of the γ-independent quantities in Eq. (26), are $g_0(\gamma) = g_0$, $g_1(\gamma) = -g_2\sin\gamma$, and $g_2(\gamma) = g_2\cos\gamma$. Putting these in Eqs. (17)–(20), we find the new interaction coefficients in terms of the old ones, viz., $J(\gamma) = J$, $D_x(\gamma) = -D_y\sin\gamma$, $D_y(\gamma) = D_y\cos\gamma$, $\gamma_{xx}(\gamma) = \gamma_{yy}\sin^2\gamma$, $\gamma_{yy}(\gamma) = \gamma_{yy}\cos^2\gamma$, and $\gamma_{xy}(\gamma) = \gamma_{yx}(\gamma) = -\gamma_{yy}\sin\gamma\cos\gamma$, and the rest of the coefficients are zero. After some matrix multiplications, one finds from Eq. (9) that the total energy $E(\vec{R})$ does not change under rotation, even though the individual interaction coefficients do change as just listed above.

A. High-Fermi-energy limit

We consider high Fermi energy ($E_F \gg m\alpha^2/\hbar^2$) and the long-distance limit for R, so that the argument x of the Hankel function in Eq. (26) is large, and the asymptotic expansion becomes

$$H_n^{(1)}(x) \simeq 2^{1/2}(\pi x)^{-1/2}\exp[i(x - n\pi/2 - \pi/4)]. \quad (27)$$

This is valid for all energy except for $E \sim 0$, where the prefactor x makes the limit $xH_n^{(1)}(x) \to x^{1/2}$, which therefore does not contribute much to the energy integrals in Eqs. (17)–(20). With this consideration, the large-x limit can be used in the entire range of energy E, and Eq. (26) yields in this limit the results

$$g_0 \simeq -i\bar{f}\exp\left[i\left(\frac{m}{\hbar^2}f(\alpha,E)R - \frac{\pi}{4}\right)\right]\cos(m\hbar^{-2}\alpha R),$$
$$g_2 \simeq \bar{f}\exp\left[i\left(\frac{m}{\hbar^2}f(\alpha,E)R - \frac{\pi}{4}\right)\right]\sin(m\hbar^{-2}\alpha R), \quad (28)$$

where $\bar{f} \equiv m^{1/2}[2\pi\hbar^2 f(\alpha,E)R]^{-1/2}$ and we have assumed $f(\alpha,E) \gg \alpha$. Putting these expressions in Eqs. (17)–(20), we immediately find the long-distance behavior

$$J = -\frac{\lambda^2 m}{8\pi^2R^2}\cos\left(\frac{2m\alpha}{\hbar^2}R\right)\sin(2q_FR), \quad (29)$$

$$\vec{D} = \hat{y}\frac{\lambda^2 m}{8\pi^2R^2}\sin\left(\frac{2m\alpha}{\hbar^2}R\right)\sin(2q_FR), \quad (30)$$

$$\gamma_{yy} = -\frac{\lambda^2 m}{8\pi^2R^2}\left[1 - \cos\left(\frac{2m\alpha}{\hbar^2}R\right)\right]\sin(2q_FR), \quad (31)$$

where

$$q_F = (m^2\alpha^2/\hbar^4 + 2mE_F/\hbar^2)^{1/2}. \quad (32)$$

This is consistent with the known results in the literature [15].

There are several things to notice from these equations. The first is that when $\alpha = 0$, one recovers the limit for the standard 2DEG results [24] for J, and the vector and tensor interactions $\vec{D}$ and $\overleftrightarrow{\Gamma}$ become zero. Second, when one takes the small α limit, one gets the result that $J \propto \alpha^0$, $\vec{D} \propto \alpha$, and $\overleftrightarrow{\Gamma} \propto \alpha^2$, which indicates the appropriate power-law dependence on the strength of the SOC α. Finally, note that Eqs. (29)–(31) show a beat pattern, which comes from the two different momentum scales in the problem, viz., the Fermi momentum for the two bands or their average q_F and the difference $2m\alpha/\hbar^2$, which appear in the equations.

To check the correctness of our approximations (27) and (28), in Fig. 2, we plot the magnitudes of the magnetic interactions computed with and without these approximations [in the latter case Eqs. (26) and (17)–(20) are used]. The similarity of these two curves confirms the approximations we have used in deriving the long-distance behavior equations (29)–(31).

B. Low-Fermi-energy limit

We consider now the limit of low Fermi energy ($|E_F - E_{\min}| \ll |E_{\min}|$) and again the long-distance limit. In this case, the electrons occupy a small circular strip, as indicated in Fig. 3, which resembles a one-dimensional system. Not surprisingly, the system shows magnetic interaction characteristics of the one-dimensional electron gas, as we shall see below. For this case, it is easy to see that

$$f(\alpha,E) \ll \alpha. \quad (33)$$

With this approximation, α can be neglected in the prefactors $f(\alpha,E) \pm \alpha$ appearing in the expressions for g_0 and g_2 in

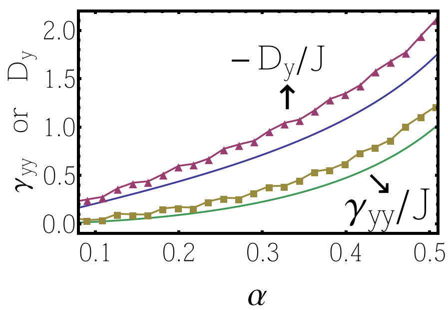

FIG. 2. Numerical results for the ratios D_y/J and γ_{yy}/J as a function of α (in eV Å) in the large-E_F and large-R limit. The points connected by lines indicate the numerical results, while the smooth lines are analytical results, Eqs. (29)–(31). Note from the same equations that the Fermi energy dependence drops out in the ratios, and here, $R = 7.5$ Å was used.

Eq. (26) but must be kept in the arguments of the Hankel functions, which will produce the characteristic oscillations of the RKKY interactions as a function of R. Once again, for the long-distance limit, the asymptotic expansion (27) for Hankel's functions can be used, leading to the result

$$g_0 \simeq -i\frac{m\alpha}{4\hbar^2}\frac{1}{\sqrt{\pi\alpha R\varepsilon}} \times \{e^{i(\sqrt{\frac{2m\varepsilon}{\hbar^2}}R+\frac{m\alpha}{\hbar^2}R-\pi/4)} + ie^{i(\sqrt{\frac{2m\varepsilon}{\hbar^2}}R-\frac{m\alpha}{\hbar^2}R-\pi/4)}\}, \quad (34)$$

$$g_2 \simeq \frac{m\alpha}{4\hbar^2}\frac{1}{\sqrt{\pi\alpha R\varepsilon}} \times \{e^{i(\sqrt{\frac{2m\varepsilon}{\hbar^2}}R+\frac{m\alpha}{\hbar^2}R-3\pi/4)} - i\, e^{i(\sqrt{\frac{2m\varepsilon}{\hbar^2}}R-\frac{m\alpha}{\hbar^2}R-3\pi/4)}\}. \quad (35)$$

In the above equations, $\varepsilon \equiv E + \frac{m\alpha^2}{2\hbar^2}$, which measures the energy with respect to the energy minimum in momentum space. Equations (17)–(20) then lead to the results in the low-Fermi-energy limit:

$$J = \frac{\lambda^2 m^2\alpha}{4\pi^2\hbar^2 R}\sin(2k_0R)\mathrm{si}(2\Delta_k R), \quad (36)$$

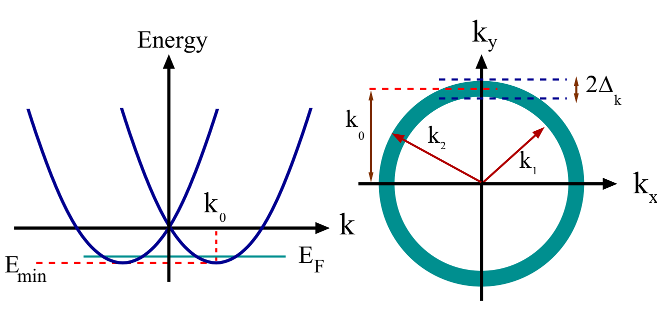

FIG. 3. Occupied momentum states in the low-E_F limit, valid for cases of both Rashba-only and Dresselhaus-only SOC. The occupied states form a thin circular strip, resembling a 1D electron gas. We have defined $\Delta_k = (k_1 - k_2)/2$ and $k_0 = (k_1 + k_2)/2$, where $k_0 = \alpha m/\hbar^2$ (Rashba) or $k_0 = \beta m/\hbar^2$ (Dresselhaus).

$$\vec{D} = -\hat{y}\,\frac{\lambda^2 m^2\alpha}{4\pi^2\hbar^2 R}\cos(2k_0R)\mathrm{si}(2\Delta_k R), \quad (37)$$

$$\gamma_{yy} = \frac{\lambda^2 m^2\alpha}{4\pi^2\hbar^2 R}[\sin(2k_0R) - 1]\mathrm{si}(2\Delta_k R), \quad (38)$$

where $\mathrm{si}(x) = \mathrm{Si}(x) - \pi/2$, with $\mathrm{Si}(x)$ being the well-known sine integral. Clearly, if $\alpha \to 0$, there are no electrons in the system, so that the magnetic interactions go to zero. Also, not surprisingly, the $\mathrm{si}(x)$ function appears here, similar to what happens in the one-dimensional (1D) case [25] since the Fermi surface forms a thin circular strip, as seen from Fig. 3. Nevertheless, at large distances $\mathrm{si}(x) \propto 1/x$, so that the magnetic interactions still fall off as $1/R^2$, the well-known decay factor for the RKKY interaction for the 2D case [24].

IV. 2DEG WITH DRESSELHAUS SPIN-ORBIT COUPLING

We consider the case when only the Dresselhaus term is present, so that the Hamiltonian is

$$H(\vec{k}) = \begin{pmatrix} \frac{\hbar^2k^2}{2m} & \beta k e^{i\theta} \\ \beta k e^{-i\theta} & \frac{\hbar^2k^2}{2m} \end{pmatrix}, \quad (39)$$

which leads to eigenstates with energies $\varepsilon_{\vec{k}\nu} = \hbar^2k^2/2m + (-1)^\nu\beta k$ and the wave functions $|\vec{k}\nu\rangle = (a^{\uparrow}_{\vec{k}\nu}, a^{\downarrow}_{\vec{k}\nu}) = 2^{-1/2}((-1)^\nu e^{i\theta}, 1)$ for $\nu = 1$ and 2, respectively. The spin eigenfunctions are indicated in the right hand part of Fig. 1. The GF coefficients for the Dresselhaus case can be expressed in terms of the same for Rashba case to yield

$$g_0^D = g_0, \quad g_1^D = -g_2, \quad g_2^D = g_3^D = 0, \quad (40)$$

where in expressions (26) for g_0 and g_2, α is to be replaced by β. Thus the algebra to get the magnetic interactions is the same as that for the Rashba case, and one finds using Eqs. (17)–(20) that the magnetic interactions between the two cases are closely related.

Explicitly, one finds, in the high-Fermi-energy, long-distance limit, the result

$$J = -\frac{\lambda^2 m}{8\pi^2R^2}\cos\left(\frac{2m\beta}{\hbar^2}R\right)\sin(2q_FR), \quad (41)$$

$$\vec{D} = -\hat{x}\,\frac{\lambda^2 m}{8\pi^2R^2}\sin\left(\frac{2m\beta}{\hbar^2}R\right)\sin(2q_FR), \quad (42)$$

$$\gamma_{xx} = -\frac{\lambda^2 m}{8\pi^2R^2}\left[1 - \cos\left(\frac{2m\beta}{\hbar^2}R\right)\right]\sin(2q_FR), \quad (43)$$

where $q_F = (m^2\beta^2/\hbar^4 + 2mE_F/\hbar^2)^{1/2}$.

Similarly, in the low-Fermi-energy, long-distance limit, we get

$$J = \frac{\lambda^2 m^2\beta}{4\pi^2\hbar^2 R}\sin(2k_0R)\mathrm{si}(2\Delta_k R), \quad (44)$$

$$\vec{D} = \hat{x}\,\frac{\lambda^2 m^2\beta}{4\pi^2\hbar^2 R}\cos(2k_0R)\mathrm{si}(2\Delta_k R), \quad (45)$$

$$\gamma_{xx} = \frac{\lambda^2 m^2\beta}{4\pi^2\hbar^2 R}[\sin(2k_0R) - 1]\mathrm{si}(2\Delta_k R). \quad (46)$$

Unlike the case of Rashba interaction in the last section, here, $\vec{D}$ is in the $\hat{x}$ direction, while only the γ_{xx} term is nonzero in the tensor term $\overleftrightarrow{\Gamma}$.

In writing expression (40), we have, like in the Rashba case, taken the distance vector $\vec{R}$ along the k_x direction. If we take $\vec{R}$ along the polar angle γ, then the expressions for the GF coefficients become $g_0^D(\gamma) = g_0^D$, $g_1^D(\gamma) = g_1^D \cos\gamma$, and $g_2^D(\gamma) = g_1^D \sin\gamma$, with the rest being zero. However, interestingly, energy $E(\vec{R})$ here also does not depend on the direction of $\vec{R}$ in the plane.

V. SPIN-POLARIZED 2DEG WITH NO RASHBA OR DRESSELHAUS TERM

Another limit in which one can obtain the long-distance behavior for the magnetic interactions is the limit where there is spin polarization, but both the Rashba and Dresselhaus SOC terms are absent, i.e., $\alpha = \beta = 0$ but $\Delta \neq 0$. This case was treated in our earlier work [20,26], and we quote the results here for completeness.

In this case, the Green's function becomes spin diagonal with the form

$$G_{\sigma\sigma}(\vec{r},\vec{r}',E) = -\frac{m}{\pi\hbar^2} K_0\left[-i\frac{\sqrt{2m}}{\hbar}|\vec{r}-\vec{r}'|\alpha(E\pm\Delta)\right], \tag{47}$$

where $+$ $(-)$ stands for $\sigma = \uparrow (\downarrow)$, K_0 is the modified Bessel function of the second kind, and

$$\alpha(x) = \begin{cases} \sqrt{x} & \text{if } x > 0, \\ i\sqrt{|x|} & \text{if } x < 0. \end{cases} \tag{48}$$

The only terms that survive are J and γ_{zz}, and the expressions are

$$J = \frac{\lambda^2 m^2}{8\pi\hbar^2}\left\{-\frac{2}{\pi}\int_{-\Delta}^{\Delta} \mathrm{Re}[K_0(\kappa R)] J_0(k_+R)\,dE + \int_{\Delta}^{E_F} [J_0(k_-R)\,Y_0(k_+R) + Y_0(k_-R)\,J_0(k_+R)]\,dE\right\},$$

$$\gamma_{zz} = \frac{\lambda^2 m}{16\pi R^2}[I'(k_{F-}R) + I'(k_{F+}R)] - J, \tag{49}$$

where $I'(x) = x^2[J_0(x)\,Y_0(x) + J_1(x)\,Y_1(x)]$. Even though the time-reversal symmetry is broken, the inversion symmetry is still present, so that the DM interaction term $\vec{D} = 0$. It can be easily shown that when the spin polarization $\Delta = 0$, the only term that survives is J, and the expression becomes the same as the result for the standard 2DEG [24].

VI. MAGNETIC INTERACTIONS IN THE GENERAL CASE

In the general case, when more than one of the three terms α, β, and Δ are nonzero, the Green's functions as well as the magnetic interactions must be calculated numerically using Eqs. (7), (13), (14), and (17)–(20). We present below some numerical results. A case of particular interest is where $\alpha = \beta$ and $\Delta = 0$, i.e., where the strengths of the Rashba and the Dresselhaus terms are the same. The system has SU(2) symmetry [27], and the Fermi surface and the spin eigenfunctions are shown in Fig. 4.

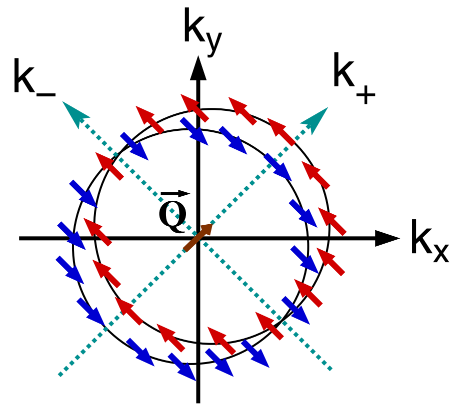

FIG. 4. The spin eigenfunctions and the Fermi surface for the case $\alpha = \beta$ and $\Delta = 0$, which consists of two circles with their centers shifted by the vector $\vec{Q} = (Q_x, Q_y) = 2\sqrt{2}m\alpha(1,1)$. The two bands are indexed by $\nu = 1$ for the outer shell and $\nu = 2$ for the inner shell.

The expressions for the eigenstates are

$$\varepsilon_{\vec{k}\nu} = \hbar^2k^2/2m + (-1)^\nu\sqrt{2}\alpha|k_x + k_y| \tag{50}$$

and

$$|\vec{k}\nu\rangle = \frac{1}{\sqrt{2}}\left[(-1)^\nu\frac{1+i}{\sqrt{2}}\,\mathrm{sgn}(k_x+k_y)|\uparrow\rangle + |\downarrow\rangle\right], \tag{51}$$

where sgn(x) is the sign function. Putting these into Eq. (14) for the GF, one finds after straightforward calculations the following results for the GF coefficients:

$$g_0 = \frac{1}{2A}\sum_{\vec{k}} e^{i\vec{k}\cdot(\vec{r}_1-\vec{r}_2)}\left(\frac{1}{E+i\mu-\varepsilon'_+} + \frac{1}{E+i\mu-\varepsilon'_-}\right),$$

$$g_2 = \frac{1}{2\sqrt{2}A}\sum_{\vec{k}} e^{i\vec{k}\cdot(\vec{r}_1-\vec{r}_2)}\left(\frac{1}{E+i\mu-\varepsilon'_+} - \frac{1}{E+i\mu-\varepsilon'_-}\right), \tag{52}$$

$$g_3 = 0, \quad g_1 = -g_2, \tag{53}$$

where $\varepsilon'_\pm = \hbar^2k^2/2m \pm \sqrt{2}\alpha(k_x+k_y)$. The general equations for the magnetic interactions (17)–(20) along with Eq. (53) lead to the results, viz., $D_x = -D_y$, $\gamma_{xx} = \gamma_{yy}$, $\gamma_{zz} = 0$ in this case, as may be seen from the computed interactions shown in Fig. 5.

VII. DOMAIN WALL ENERGETICS

As mentioned already, it is increasingly being realized that the DM interactions have an important effect in determining the domain wall structures in magnetic materials, particularly for ultrathin films, where surface and bulk inversion asymmetries lead to the Rashba and Dresselhaus SOC terms, which in turn lead to the DM interactions. In an earlier work, Chen *et al.* [6] observed the formation of the Néel wall with a definite chirality in magnetized Ni/Co film, which was surprising since the Bloch wall usually has a lower energy. This was attributed to the existence of a strong DM interaction in the film. Furthermore, by interface engineering, they were able to adjust the DM

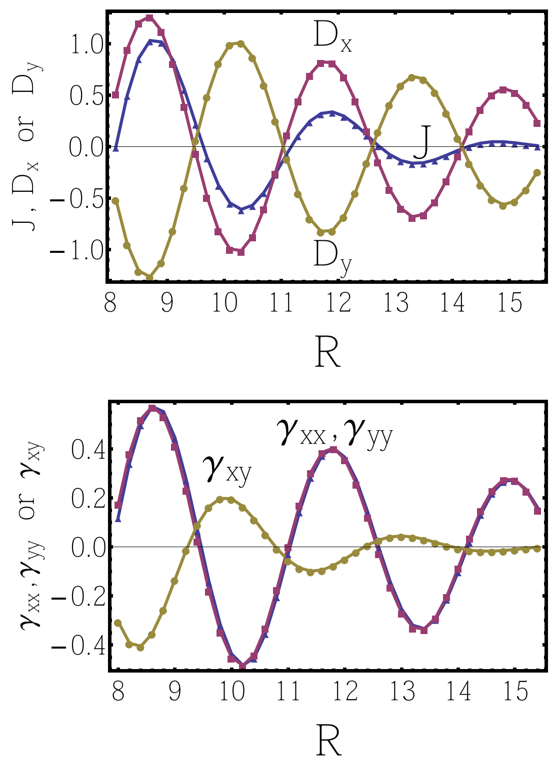

FIG. 5. Computed magnetic interactions for equal Rashba and Dresselhaus SOCs and $\Delta = 0$. Here, $E_F = 3.4$ eV, $\alpha = \beta = 0.22$ eV Å, distance R is in angstroms, and the magnetic interactions are in units of $10^{-4}\,\lambda^2 m$.

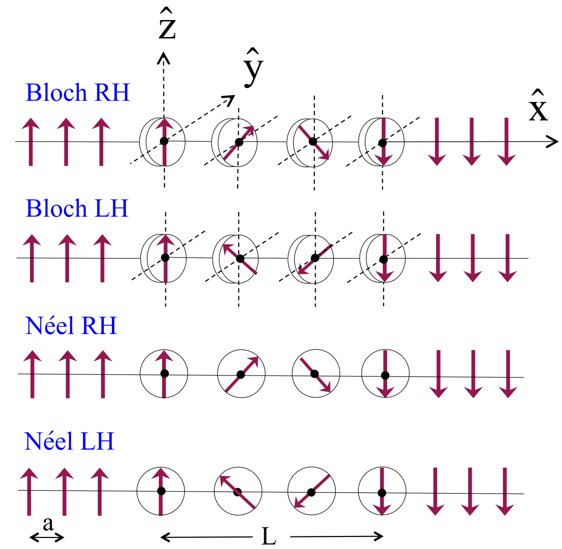

FIG. 6. Bloch and Néel walls, right (RH) and left (LH) handed.

interaction and stabilize either the left-handed or the right-handed Néel walls or nonchiral Bloch walls. In a more recent experiment, Di *et al.* [13] were able to directly measure a strong DM interaction in Pt/Co/Ni thin-film structures using Brillouin spectroscopy. In addition, the strength of the DM interactions can be controlled by external means. For example, we have recently shown from *ab initio* calculations that the Rashba SOC can be tuned at the surface by an applied electric field [22]. Our work below does not refer to any specific material, but we make a few general observations on the domain wall energy based on our results in previous sections.

We consider the domain walls in ferromagnetic structures and the change in the wall energy due to the DM interactions. As first pointed out by Bloch [28], the domain wall thickness is determined by a competition between the exchange and the anisotropy energy. The wall structure, discussed in the seminal paper [29] by Landau and Lifshitz, is determined by optimizing the total energy $E = \int_{-\infty}^{\infty} (A\dot{\theta}^2 - B\cos^2\theta)\, dx$, subject to the boundary conditions $\theta(-\infty) = 0$ and $\theta(\infty) = \pi$, where A is the exchange stiffness, B is the anisotropy constant, $\theta(x)$ is the spin orientation across the domain wall, and $\dot{\theta} \equiv d\theta/dx$. The structure of the wall, obtained by solving the corresponding Euler-Lagrange equations, is given by

$$\theta(x) = 2\tan^{-1}\exp(2x/L), \tag{54}$$

where $L = 2(A/B)^{1/2}$ is the width of the wall and the result $\dot{\theta}(x) = \sqrt{B/A}\sin\theta(x)$ is used later in calculating the domain wall energy. We assume that the wall thickness does not change due to the DM interactions, which is reasonable because the DM interactions are considerably weaker than the exchange and anisotropy energies, which determine the width of the domain wall.

The spin orientations (see Fig. 6) for the Néel and Bloch walls, $\hat{S}_N^{R,L}(x)$ and $\hat{S}_N^{R,L}(x)$, where R (L) refers to the right-handed (left-handed) wall, are given by

$$\begin{aligned} \hat{S}_N^{R,L}(x) &= \cos\theta(x)\hat{z} \pm \sin\theta(x)\hat{x}, \\ \hat{S}_B^{R,L}(x) &= \cos\theta(x)\hat{z} \pm \sin\theta(x)\hat{y}. \end{aligned} \tag{55}$$

We compute the extra wall energy due to the DM terms for different walls from the total energy expression (9) and the wall structure Eq. (54) and by keeping the dominant nearest-neighbor DM interactions for simplicity. The integrations are straightforward, leading to the desired result

$$\begin{aligned} \frac{E_N^{R,L}}{S^2} &= -\frac{J}{N_w} \pm \pi D_y + \frac{N_w}{2}(\gamma_{xx} - \gamma_{zz}) + \frac{3\gamma_{xx} - \gamma_{zz}}{4N_w}, \\ \frac{E_B^{R,L}}{S^2} &= -\frac{J}{N_w} \mp \pi D_x + \frac{N_w}{2}(\gamma_{yy} - \gamma_{zz}) + \frac{3\gamma_{yy} - \gamma_{zz}}{4N_w}, \end{aligned} \tag{56}$$

where $N_w = L/a$ is the size of the wall, the upper (lower) sign in $\pm$ or $\mp$ refers to the right- (left-) handed wall, and the interactions J, D_x, D_y, γ_{ii} are between nearest neighbors. Comparing the relative energies of the two walls, we get

$$\begin{aligned} \varepsilon_N^{R,L} &= \pm\pi D_y + c\,\gamma_{xx}, \\ \varepsilon_B^{R,L} &= \mp\pi D_x + c\,\gamma_{yy}, \end{aligned} \tag{57}$$

where $c = 2^{-1}N_w + 3(4N_w)^{-1}$ is a constant. The type of wall that forms in the structure depends on the minimum of these energies. The result, Eq. (57), clearly shows that the helicity of the wall simply depends on the sign of the DM interaction $\vec{D}$, while the type of wall (Bloch or Néel) depends on both the vector and tensor DMI, $\vec{D}$ and $\overleftrightarrow{\Gamma}$. Since the DMI is controlled by the strengths of the Rashba and

Dresselhaus SOCs, these results suggest the possibility of tailoring the domain wall structures by modifying the Rashba and Dresselhaus interactions by interface engineering or by applying an external gate voltage.

VIII. SUMMARY

In summary, we studied the Dzyaloshinskii-Moriya interaction in the presence of Rashba and Dresselhaus spin-orbit coupling for a spin-polarized electron gas and obtained some general conclusions for domain wall structures in magnetic thin films. General expressions for the RKKY and DM interactions (J, $\vec{D}$, and $\overleftrightarrow{\Gamma}$), valid irrespective of the dimensionality of the system, were obtained as integrals over the Pauli expansion coefficients of the Green's function [Eq. (10)].

Using these expressions, we obtained the analytical expressions for the magnetic interactions in the long-distance limit for specific cases, viz., when only the Rashba or Dresselhaus interaction is present in both the high- and low-Fermi-energy limits. Our results agree with the limits that were already obtained in the literature, viz., the high-Fermi-energy case. The low-Fermi-energy limit, where the electrons occupy a thin circular strip in the momentum space, shows 1D-like behavior for the magnetic interactions.

Finally, we examined the energetics of the Bloch and Néel domain walls and obtained general expressions that suggest how the magnetic domain wall structures can be tailored by controlling the relative strengths of the Rashba and the Dresselhaus terms. Such control may be achieved by interface engineering, as has been demonstrated for semiconductor quantum well structures and/or by the application of a gate voltage.

ACKNOWLEDGMENTS

We thank the US Department of Energy, Office of Basic Energy Sciences, Division of Materials Sciences and Engineering for financial support under Grant No. DE-FG02-00ER45818.

[1] M. A. Ruderman and C. Kittel, Indirect exchange coupling of nuclear magnetic moments by conduction electrons, Phys. Rev. **96**, 99 (1954).

[2] T. Kasuya, A theory of metallic ferro- and antiferromagnetism on Zener's model, Prog. Theor. Phys. **16**, 45 (1956).

[3] K. Yosida, Magnetic properties of Cu-Mn alloys, Phys. Rev. **106**, 893 (1957).

[4] I. Dzyaloshinskii, A thermodynamic theory of a "weak" ferromagnetism of antiferromagnetics, J. Phys. Chem. Solids **4**, 241 (1958).

[5] T. Moriya, Anisotropic superexchange interaction and weak ferromagnetism, Phys. Rev. **120**, 91 (1960).

[6] G. Chen, T. Ma, A. T. N'Diaye, H. Kwon, C. Won, Y. Wu, and A. K. Schmid, Tailoring the chirality of magnetic domain walls by interface engineering, Nat. Commun. **4**, 2671 (2013).

[7] A. Soumyanarayanan *et al.*, Tunable room temperature magnetic skyrmions in Ir/Fe/Co/Pt multilayers, Nat. Mater. **16**, 898 (2017).

[8] E. I. Rashba, Cyclotron and combinational resonance in a magnetic field perpendicular to the plane of the loop, Sov. Phys. Solid State **2**, 1109 (1960).

[9] G. Dresselhaus, Spin-orbit coupling effects in zinc blende structures, Phys. Rev. **100**, 580 (1955).

[10] J. Nitta, T. Akazaki, H. Takayanagi, and T. Enoki, Gate Control of Spin-Orbit Interaction in an Inverted $In_{0.53}Ga_{0.47}As/In_{0.52}Al_{0.48}As$ Heterostructure, Phys. Rev. Lett. **78**, 1335 (1997).

[11] P. Lyu, N.-N. Liu, and C. Zhang, Gate-tunable Ruderman-Kittel-Kasuya-Yosida interaction mediated by low-dimensional electrons with Rashba spin-orbit coupling, J. Appl. Phys. **102**, 103910 (2007).

[12] J. Yu, X. Zheng, S. Cheng, Y. Chen, Y. Liu, Y. Lai, Q. Zheng, and J. Ren, Tuning of Rashba/Dresselhaus spin splittings by inserting ultra-thin InAs layers at interfaces in insulating GaAs/AlGaAs quantum wells, Nanoscale Res. Lett. **11**, 477 (2016).

[13] K. Di, V. L. Zhang, H. S. Lim, S. C. Ng, and M. H. Kuok, Direct Observation of the Dzyaloshinskii-Moriya Interaction in a Pt/Co/Ni Film, Phys. Rev. Lett. **114**, 047201 (2015).

[14] S. Datta and B. Das, Electronic analog of the electrooptic modulator, Appl. Phys. Lett. **56**, 665 (1990).

[15] H. Imamura, P. Bruno, and Y. Utsumi, Twisted exchange interaction between localized spins embedded in a one- or two-dimensional electron gas with Rashba spin-orbit, Phys. Rev. B **69**, 121303 (2004).

[16] D. F. Mross and H. Johannesson, Two-impurity Kondo model with spin-orbit interactions, Phys. Rev. B **80**, 155302 (2009).

[17] S. Chesi and D. Loss, RKKY interaction in a disordered two-dimensional electron gas with Rashba and Dresselhaus spin-orbit couplings, Phys. Rev. B **82**, 165303 (2010).

[18] K.-W. Kim, H.-W. Lee, K.-J. Lee, and M. D. Stiles, Chirality from Interfacial Spin-Orbit Coupling Effects in Magnetic Bilayers, Phys. Rev. Lett. **111**, 216601 (2013).

[19] A. Kundu and S. Zhang, Dzyaloshinskii-Moriya interaction mediated by spin-polarized band with Rashba, Phys. Rev. B **92**, 094434 (2015).

[20] For a pedagogical derivation of the interaction energy, see M. Valizadeh and S. Satpathy, Magnetic exchange interaction in the spin-polarized electron gas, Phys. Status Solidi B **253**, 2245 (2016); M. Valizadeh, Anisotropic Heisenberg form of RKKY interaction in the one-dimensional spin-polarized electron gas, Int. J. Mod. Phys. B **30**, 1650234 (2016).

[21] R. Winkler, *Spin-Orbit Effects in Two-Dimensional Electron and Hole Systems* (Springer, New York, 2003).

[22] K. V. Shanavas and S. Satpathy, Electric Field Tuning of the Rashba Effect in the Polar Perovskite Structures, Phys. Rev. Lett. **112**, 086802 (2014).

[23] I. S. Gradshteyn and I. M. Ryzhik, *Tables of Integrals, Series, and Products* (Academic, New York, 1980), Sec. 8.511.4.

[24] B. Fischer and M. W. Klein, Magnetic and nonmagnetic impurities in two-dimensional metals, Phys. Rev. B **11**, 2025 (1975).

[25] Y. Yafet, Ruderman-Kittel-Kasuya-Yosida range function of a one-dimensional free-electron gas, Phys. Rev. B **36**, 3948 (1987).

[26] M. Valizadeh and S. Satpathy, RKKY interaction for the spin-polarized electron gas, Int. J. Mod. Phys. B **29**, 1550219 (2015).

[27] B. A. Bernevig, J. Orenstein, and S.-C. Zhang, Exact SU(2) Symmetry and Persistent Spin Helix in a Spin-Orbit Coupled System, Phys. Rev. Lett. **97**, 236601 (2006).

[28] F. Bloch, Zur Theorie des Austauschproblems und der Remanenzerscheinung der Ferromagnetika, Z. Phys. **74**, 295 (1932).

[29] L. D. Landau and E. M. Lifshitz, On the Theory of the Dispersion of magnetic permeability in ferromagnetic bodies, Phys. Z. Sowjetunion **8**, 153 (1935).